

# Study of a central force model for liquid water by molecular dynamics\*

A. Rahman

Argonne National Laboratory, Argonne, Illinois 60439

F. H. Stillinger and H. L. Lemberg

Bell Laboratories, Murray Hill, New Jersey 07974

(Received 16 June 1975)

The simulation technique of molecular dynamics has been used to investigate a central-force model for liquid water at 22°C and 1 g/cm<sup>3</sup>. In this model, the same atomic pair potentials are used both for intramolecular and intermolecular interactions. Atomic pair correlation functions and velocity autocorrelation functions have been computed. The results demonstrate that stable, nonlinear, vibrating molecules are present, and that they form a random hydrogen-bond network of the type usually attributed to water. These exploratory calculations suggest that small modifications in the central potentials  $V_{HH}$ ,  $V_{OH}$ , and  $V_{OO}$  would produce a more faithful representation of real water.

## I. INTRODUCTION

Computer simulation has recently emerged as a powerful tool for the study of water<sup>1-5</sup> and aqueous solutions.<sup>6,7</sup> This technique has already demonstrated modest success in predicting experimental results for both kinetic and structural properties at the molecular level, as well as thermodynamic properties at the macroscopic level. Furthermore, it has supplied types of information about aqueous fluids that are entirely unavailable through measurements on real substances, e.g., the distribution of hydrogen-bond polygons.<sup>8</sup> It seems likely that computer simulation for water will improve in breadth and precision, as well as increase in frequency.

In the simulations pursued thus far, the water molecules have been treated as rigid asymmetric rotors subject to strongly anisotropic (but pairwise additive) interactions. Unfortunately, the conventional analytical theory for liquids is confined largely to spherical, or nearly spherical, molecules. Hence, *ab initio* theory for water and aqueous solutions has been unable to keep pace with direct computer simulation.

In addition, it seems desirable eventually to incorporate nonadditive intermolecular interactions into the simulations, since accurate quantum-mechanical calculations of potential energy surfaces for water aggregates<sup>9,10</sup> suggest that nonadditive interactions are important in the liquid. Once again, conventional liquid theory is ill suited to handle this feature.

Therefore, in the case of water we are faced with the prospect of an ever-widening gap between experiment and computer simulation on the one hand, and fundamental statistical mechanics for liquids on the other hand. In an effort to narrow such a gap, a conceptually simple class of "central force models" for water has been proposed.<sup>11,12</sup> These models postulate a set of three central potentials,  $V_{HH}(r)$ ,  $V_{OH}(r)$ , and  $V_{OO}(r)$ , which together describe *all* atom-pair interactions in the system, whether or not the atoms belong to the same molecule. Thus, water is regarded as a binary mixture of spherical particles, so that if the model works, it should be possible to apply the known methods of analyt-

ical theory (at least in some temperature-density ranges).

The functions  $V_{HH}$ ,  $V_{OH}$ , and  $V_{OO}$  can be chosen so that H+H+O triads spontaneously settle into the nonlinear geometry required for separate H<sub>2</sub>O molecules. Subsequently, pairs of the resulting water molecules can be made to engage in linear hydrogen bonds by proper balance between the nine competing intermolecular force contributions.

The pre-eminent advantages of the central force models are that (a) intramolecular vibrations are included; (b) molecular dissociation into H<sup>+</sup> and OH<sup>-</sup> and recombination are possible; (c) as mentioned above, exclusive use of central forces facilitates application of conventional liquid-state theory to these models; and (d) it is also noteworthy that molecular distortion occurs as molecules interact, and this automatically provides a source of some nonadditive interaction between molecules.

The mathematical requirement that only additive central forces between atoms be present, will probably limit "central force water" to modest precision in comparison with experiment. However, all of the important qualitative features seem to be present, some for the first time. Central force models bear roughly the same relation to water chemistry and physics that the venerable (but often imprecise) Ising model bears to the general study of phase transitions.<sup>13</sup>

The present paper reports results of a molecular dynamics investigation into one version of the central force models. Although it is clear that the specific choice of  $V_{HH}$ ,  $V_{OH}$ , and  $V_{OO}$  is not optimal, the results are nevertheless quite encouraging. In the light of these results, we believe that central force models should be investigated not only for water, but for other polyatomic substances as well.

Application of known integral equation methods to the central force models for water will be reported separately.

## II. CENTRAL FORCE INTERACTIONS

The specific central interactions used in the present study have the following functional forms (using kcal/mole and Å as energy and length units):

$$V_{\text{HH}}(r) = \frac{36.1345}{r} + \frac{20}{1 + \exp[40(r-2)]} - 17.03002 \exp[-7.60626(r-1.4525)^2]; \quad (2.1)$$

$$V_{\text{OH}}(r) = -\frac{72.269}{r} + \frac{2.6677}{r^{14.97}} - \frac{6}{1 + \exp[5.49305(r-2.2)]}; \quad (2.2)$$

$$V_{\text{OO}}(r) = \frac{144.538}{r} + \frac{23401.9}{r^{6.3827}}. \quad (2.3)$$

Figure 1 displays these functions graphically. Although they differ in some quantitative details from the set advocated in Refs. 11 and 12, the dominant features remain unchanged.

Only  $V_{\text{HH}}$  and  $V_{\text{OH}}$  contribute to the potential energy surface for an isolated water molecule.  $V_{\text{HH}}$  possesses a relative minimum at 1.5151 Å, while  $V_{\text{OH}}$  possesses an absolute minimum at 0.9584 Å; in the  $\text{H}_2\text{O}$  "aggregate," these distances are automatically attained at a mechanical equilibrium geometry, which we have chosen to be that experimentally determined for the isolated molecule.

Given the molecular geometry, and 1.86 D as the measured dipole moment for the isolated molecule, the hydrogen atoms must be assigned charge 0.32983  $e$ , and the oxygen atoms must bear charge -0.65966  $e$ . These assignments underlie the Coulombic terms in each of Eqs. (2.1), (2.2), and (2.3).

The potentials  $V_{\text{HH}}$ ,  $V_{\text{OH}}$ , and  $V_{\text{OO}}$  are such that the net interaction between two  $\text{H}_2\text{O}$  triads leads to formation of a linear hydrogen bond. Although the molecules participating in such a dimer would tend to distort, calculations indicate that the effect is small.<sup>12</sup> In the absence of such distortion, two  $\text{H}_2\text{O}$  triads can lower their

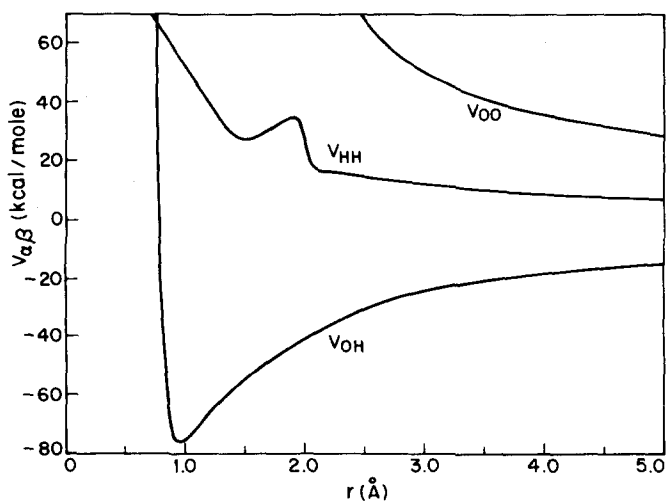


FIG. 1. Central potentials used for all atom pairs in the present model for water. The specific functions plotted here appear in Eqs. (2.1)–(2.3).

TABLE I. Water molecule normal mode frequencies.<sup>a</sup>

Mode	$\text{H}_2\text{O}^{16}$		$\text{D}_2\text{O}^{16}$	
	CF model	Experiment <sup>b</sup>	CF model	Experiment <sup>b</sup>
Asymmetric stretch	3805.10	3755.79	2788.05 <sup>c</sup>	2788.05
Symmetric stretch	4266.01	3656.65	3057.09	2671.46
Symmetric bend	1369.33	1594.59	1008.20	1178.33

<sup>a</sup>Frequencies in  $\text{cm}^{-1}$ .

<sup>b</sup>D. Eisenberg and W. Kauzmann, *The Structure and Properties of Water* (Oxford U. P., New York, 1969), pp. 7–8.

<sup>c</sup>Chosen to agree exactly with experiment.

energy by -6.12 kcal/mole by forming an optimal hydrogen bond, for which the oxygen–oxygen separation is 2.86 Å.

Three vibrational normal modes exist for each molecule. Their frequencies (for free molecules) depend on curvatures of  $V_{\text{HH}}$  and  $V_{\text{OH}}$ , only at the positions of mechanical equilibrium. Because these two adjustable parameters would not permit simultaneous fit to all three experimental frequencies, a compromise was adopted. The curvature values

$$V''_{\text{HH}}(1.5151) = 257.25 \text{ kcal/mole} \cdot \text{Å}^2, \quad (2.4)$$

$$V''_{\text{OH}}(0.9584) = 1147.65 \text{ kcal/mole} \cdot \text{Å}^2$$

were selected first to reproduce the asymmetric stretch frequency in  $\text{D}_2\text{O}$ , and then to equalize fractional errors (at 14.4%) in the two symmetric mode frequencies for the same molecule. Table I provides a compilation of normal mode frequencies, both experimental and calculated for the central force model, with  $\text{H}_2\text{O}$  and  $\text{D}_2\text{O}$ .

The set of potentials (2.1)–(2.3) contains an inadvertent weakness that needs to be (and easily can be) removed. Besides the desired nonlinear  $\text{H}_2\text{O}$  structure, they also produce an additional minimum for these three atoms. This spurious minimum requires the molecule to straighten out to a symmetric linear form, with OH bond lengths equal to 1.035 Å. In fact, this linear structure lies 5.376 kcal/mole lower than the realistic bent structure.<sup>14</sup> However, its presence is inconsequential in the present exploratory study, for a sufficiently large barrier ( $\approx 7.5$  kcal/mole) exists to prevent each molecule from linearizing under the conditions studied. Having started all molecules out near the bent-structure minima, they retain that structure during the course of the molecular dynamics run.

In future studies we will use modified potentials which cause the bent structure to be the absolute minimum.

## III. MOLECULAR DYNAMICS PROCEDURE

Our calculations employ 648 particles (432 hydrogens plus 216 oxygens) out of which 216 intact water molecules can be formed. These particles reside in a cubical unit cell 18.62 Å on a side, so that the mass density is  $\text{lg/cm}^3$ . Periodic boundary conditions apply; as any particle moves outward across a face of the unit cell, an image particle moves inward across the opposite face.

We use a rapid digital computer<sup>15</sup> to solve classical

(Newtonian) equations of motion for the particles, subject to forces implied by the central potentials (2.1)–(2.3). Since the particles carry permanent charges, interactions have long range. It was thought to be necessary, therefore, to include interactions with periodic images of all orders through an Ewald summation. Some technical details are indicated briefly in the Appendix. We believe that this technique is properly designed to handle long-wavelength electrostatic field fluctuations in the system that may be important for dielectric response.

To start the molecular dynamics calculation, an initial configuration for the 648 nuclei was selected from an earlier molecular dynamics study which utilized rigid water molecules.<sup>3</sup> This configuration placed each H<sub>2</sub>O triad close to the intramolecular potential minimum produced by  $V_{OH}$  and  $V_{HH}$ . As mentioned earlier, each molecule remained near this local minimum during the subsequent dynamics.

It is not surprising that when a new potential energy function (in this case the central force model) is grafted onto an instantaneous configuration corresponding to a completely different interaction scheme (rigid-molecule model), the system finds itself in a state of "discomfort," i. e., in a state of high potential energy. When the dynamical calculation is started in this manner, the system heats up rapidly at the expense of the potential energy, and the momenta need to be scaled downward several times by appropriate amounts to achieve a dynamical system in the neighborhood of room temperature. This kind of initial manipulation is standard procedure in the technique of molecular dynamics.

On account of the strong forces present in the system, and the fact that hydrogens have such small masses, a rather small time step  $\Delta t$  is required for numerical integration of the dynamical equations. We have used

$$\Delta t = 5 \times 10^{-16} \text{ sec} \quad (3.1)$$

in the present study. Even though rapid intramolecular vibrations are now present,  $\Delta t$  is roughly twice as long as the step length that has been used in prior rigid-molecule studies.<sup>3</sup> Although repeated evaluations of Ewald sums (as indicated in the Appendix) are necessary in the present case, computer running speed for a given number of molecules is somewhat faster with the present model than it was with rigid water molecules.

The single dynamical run upon which results have been based spanned 1988  $\Delta t$ , or approximately  $10^{-12}$  sec. This includes many vibrational periods for the molecular normal modes, even for the low-frequency symmetric-bend mode. The temperature during this run was 295.4 °K (22.2 °C), obtained from the mean kinetic energy per particle.

The mean potential energy per molecule was found to be -133.720 kcal/mole in the liquid relative to separated atoms. Most of this can be attributed to the bonding energy within the molecule, which is -125.400 kcal/mole at the mechanical equilibrium configuration. Thermally induced harmonic vibrations for the free molecule at 295.4 °K bring the latter value up (by  $3k_B T/2$ )

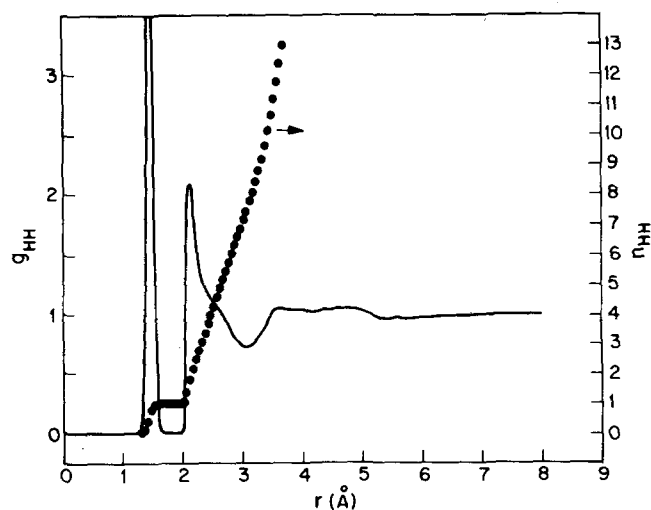


FIG. 2. Hydrogen-hydrogen pair correlation function ( $g_{HH}$ ) and its running coordination number ( $n_{HH}$ ) for the central-force model. The ambient conditions are 22 °C and 1 g/cm<sup>3</sup>.

to -124.519 kcal/mole. Thus, the mean interaction energy in the liquid is -9.201 kcal/mole. This last value compares reasonably well with the result -9.96 kcal/mole that can be calculated for real water at the same temperature, using measured thermodynamic properties.

#### IV. PAIR DISTRIBUTION FUNCTIONS

The three nuclear pair correlation functions  $g_{HH}(r)$ ,  $g_{OH}(r)$ , and  $g_{OO}(r)$  have special significance in the present context. Owing to the fact that only additive central forces are present, these correlation functions suffice to give (as suitable integrals) an important collection of equilibrium properties for the system. Included are the energy, virial pressure, isothermal compressibility, and the wavelength-dependent static dielectric response.<sup>11,12</sup> Since  $g_{HH}$ ,  $g_{OH}$ , and  $g_{OO}$  also convey important information about the packing geometry of molecules in the liquid, it is natural that these functions should be among the first quantities examined in a molecular dynamics study.

Figures 2, 3, and 4 display, respectively, the numerical results for  $g_{HH}$ ,  $g_{OH}$ , and  $g_{OO}$ . Running coordination numbers  $n_{HH}$ ,  $n_{OH}$ , and  $n_{OO}$  have been included, where

$$n_{\alpha\beta}(r) = 4\pi c_{\beta} \int_0^r s^2 g_{\alpha\beta}(s) ds \quad (4.1)$$

( $c_{\beta}$  is the number density for species  $\beta$ ); notice that in the case of  $n_{OH}$ , hydrogens surrounding a given central oxygen are counted, not the reverse.

Intramolecular structure is obvious in  $g_{HH}$  and  $g_{OH}$  as completely resolved peaks at short distance. The respective running coordination numbers rise to just the correct values over these peaks (1 for  $n_{HH}$ , 2 for  $n_{OH}$ ) to demonstrate that all 216 molecules remain intact and nonlinear. No doubt owing to strong fluctuating intermolecular forces, these intramolecular correlation peaks are substantially wider than they would be for

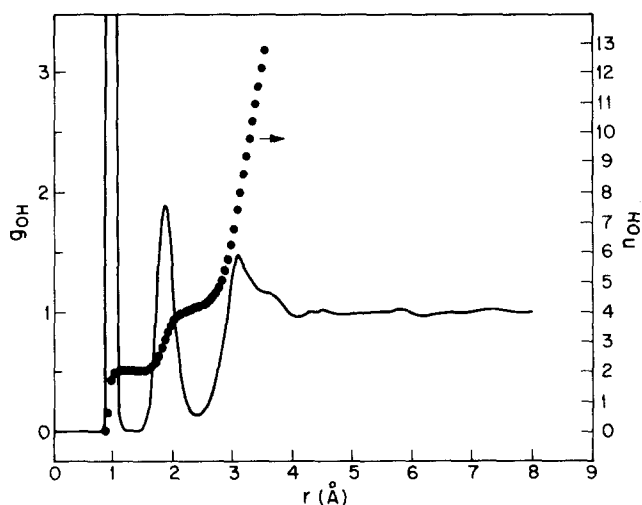


FIG. 3. Oxygen-hydrogen pair correlation function ( $g_{OH}$ ) and its running coordination number ( $n_{OH}$ ) for central force water at 22 °C and 1g/cm<sup>3</sup>.

thermally excited, but noninteracting, molecules. Furthermore, the H-H peak maximum is displaced slightly from the distance at which the corresponding pair potential achieves its minimum; the most probable bond length is about 1.46 Å. Although the O-H intramolecular peak exhibits less of a shift in its maximum (if any), the over-all shape is distinctly asymmetric.

The intramolecular correlation implicit in  $g_{OO}(r)$ , Fig. 4, is particularly significant. The shell of first neighbors centered at 2.80 Å comprises an average of 4.5 oxygens, at least as judged by  $n_{OO}(r)$  at the position of the subsequent  $g_{OO}$  minimum. This mean coordination number is only slightly larger than the 4 suggested by the structure of ice, and agrees with values determined for real water by x-ray diffraction experiments.<sup>16</sup> It is distinctly smaller than mean coordination numbers determined for simple liquids such as Ar.<sup>1</sup>

The second  $g_{OO}$  maximum is low, broad, and centered

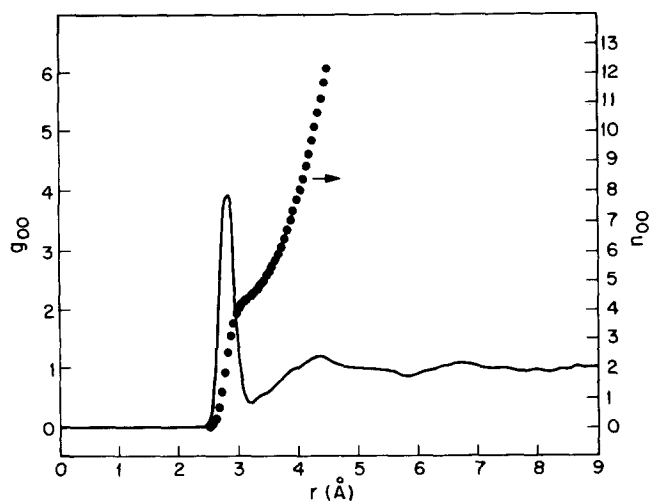


FIG. 4. Oxygen-oxygen pair correlation function ( $g_{OO}$ ) and its running coordination number ( $n_{OO}$ ) for central force water at 22 °C and 1 g/cm<sup>3</sup>.

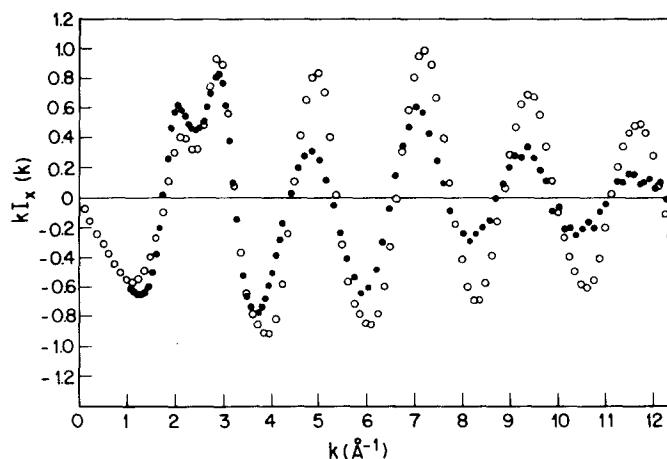


FIG. 5. Comparison between experimental (black circles) and theoretical (open circles) x-ray diffraction intensities for water. The experimental points are due to Narten, Ref. 18.

at 4.4 Å. The distance ratio, 1.57, of second to first maximum distances is sufficiently close to the ice lattice value, 1.63, to suggest that more than a vestige of icelike structure may be present. In particular, it suggests that successive linear hydrogen bonds at roughly the ideal tetrahedral angle 109.5° may persist into the liquid phase. This also agrees with conclusions based on x-ray diffraction experiments.<sup>16,17</sup>

The existence of linear hydrogen bonds in the liquid is supported by the well-resolved intermolecular  $g_{OH}$  maximum centered at 1.85 Å. The running coordination number indicates that this comprises about 2 hydrogens, just the number that would be donated to the central oxygen in linear hydrogen bonds in a tetrahedral network. Furthermore, the observed mean O-H distance lies close to that expected in such hydrogen bonds.<sup>12</sup>

Aside from the intramolecular parts, the correlation functions in Figs. 2-4 are qualitatively similar to prior molecular dynamics determinations of the same quantities that have been carried out with rigid-molecule assumptions.<sup>1-3</sup> Nevertheless, there are numerous quantitative differences whose importance is difficult to assess at present. Eventually it will be helpful to have in hand experimentally separated pair correlation functions with which direct comparisons can be carried out.

Reliable atomic structure factors are available for oxygen and hydrogen, for use in relating experimental x-ray diffraction intensities to nuclear pair correlation functions.<sup>18</sup> We have used these structure factors along with molecular dynamics results for  $g_{HH}$ ,  $g_{OH}$ , and  $g_{OO}$  to calculate the hypothetical x-ray diffraction pattern for central-force water. Figure 5 compares that pattern for 22 °C with Narten's measurements on H<sub>2</sub>O at 20 °C.<sup>18</sup> Similarly, we have employed known nuclear scattering lengths<sup>19</sup> to calculate the hypothetical neutron diffraction pattern for central-force water (with hydrogens regarded as deuterium atoms). Figure 6 shows how this pattern compares with Narten's experimental neutron diffraction pattern for D<sub>2</sub>O at 25 °C.<sup>19</sup>

The most significant feature demonstrated in Fig. 5

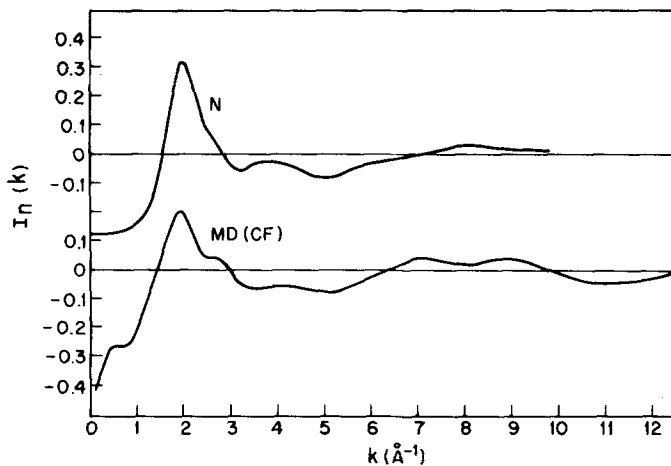


FIG. 6. Comparison between experimental (N) and theoretical (MD) neutron diffraction intensities for  $D_2O^{16}$ . The experimental curve has been taken from Narten, Ref. 19.

is the capacity of the central-force model to produce a double peak around  $2.5 \text{ \AA}^{-1}$ . This characteristic appears prominently in the experimental diffraction pattern at low temperatures, but deforms to a single maximum upon heating the water to  $200^\circ\text{C}$ .<sup>18</sup> It is hardly surprising that successive zeros for experimental and theoretical curves in Fig. 5 should agree closely, since both depend primarily on the O-O near-neighbor distance; one of the conditions used in constructing the central-force model was the observed length for linear hydrogen bonds in water. That the theoretical curve oscillates with considerably greater amplitude than its experimental counterpart indicates that O-O nearest neighbors are too narrowly distributed in distance.

The neutron diffraction curves shown in Fig. 6 exhibit good qualitative agreement. These results are considerably more sensitive to the positions of hydrogen (deuterium) atoms than are the x-ray results. Consequently, the fact that both neutron curves have maxima at  $2.0 \text{ \AA}^{-1}$  suggest that the length scale for O-H and H-H correlations is about right. The failure of the molecular dynamics maximum to reach any higher than about  $\frac{2}{3}$  the experimental height has no obvious explanation, but this weakness also occurs for rigid-molecule simulations.<sup>3</sup> The most obvious shortcoming of the calculated results in Fig. 6 is the falloff with declining  $k$  below  $0.5 \text{ \AA}^{-1}$ ; this probably arises from inadequate configurational averaging for protons, bearing in mind that the measured dielectric relaxation time at  $22^\circ\text{C}$ <sup>20</sup> is about 10 times the length ( $10^{-12}$  sec) of the molecular dynamics reported here.

## V. NUCLEAR MOTIONS

Motions of the separate nuclei in the water model are a composite of molecular vibration, rotation, and translation. There are several ways in which the motions generated during the molecular dynamics calculation can be analyzed. One of the most convenient employs velocity autocorrelation functions ( $\alpha = \text{H, O}$ ):

$$A_\alpha(t) = \langle \mathbf{v}_{\alpha j}(0) \cdot \mathbf{v}_{\alpha j}(t) \rangle / \langle \mathbf{v}_{\alpha j}^2 \rangle. \quad (5.1)$$

Here we have let  $\mathbf{v}_{\alpha j}$  stand for the velocity of the  $j$ th particle of species  $\alpha$ . The averaging implied in Eq. (5.1) uses dynamical data for all particles of the required type, and uses all available pairs of system states separated by time interval  $t$ .

Figure 7 presents the velocity autocorrelation function for oxygen. Obviously, considerable oscillatory character is present. These oscillations represent motions of the water molecules as a whole, rather than the much quicker normal mode vibration (roughly 10 times as fast). The tendency for  $A_0(t)$  to plunge from the initial value 1.0 to  $-0.1$ , followed by a positive maximum, has also been observed in earlier rigid-molecule water simulations.<sup>1-3</sup> However, in the present case these features develop in only about  $\frac{2}{3}$  the time exhibited by those rigid-molecule results. Furthermore, there seems to be less indication in the present model compared to those prior results for oscillatory behavior beyond these small-time features.

Provided that all potentials present are continuous, velocity autocorrelation functions in an equilibrium ensemble should have vanishing initial slope,

$$\lim_{\epsilon \rightarrow 0} A'_\alpha(\epsilon^2) = 0. \quad (5.2)$$

That mathematical condition is certainly satisfied by the central-force potentials (2.1)–(2.3). Nevertheless, the initial behavior shown in Fig. 7 for  $A_0(t)$  seems to involve a negative initial slope. This latter behavior is characteristic of systems in which rigid cores are present.<sup>21</sup> Evidently, the steep rise displayed by  $V_{\text{OH}}(r)$  inside its minimum (see Fig. 1) plays the role of a rigid core, at least on the time scale shown in Fig. 7.

Figure 8 shows the initial portion of  $A_0(t)$ , but with its time scale expanded by a factor of 10. It now becomes clear that the slope starts at zero. The expected leading quadratic behavior seems to be confined to about the first  $10^{-15}$  sec. A slight undulation is visible in the curve of Fig. 8, which probably represents small vibrational motion of the oxygens as the molecules execute their perturbed normal modes of vibration.

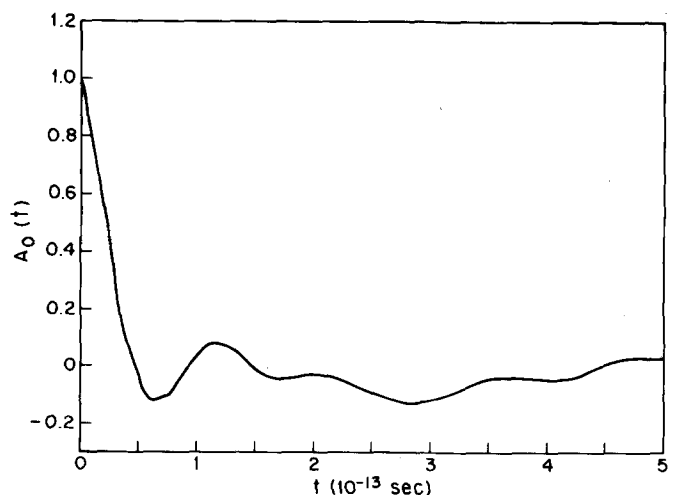


FIG. 7. Velocity autocorrelation function for oxygen particles in the central force model ( $22^\circ\text{C}$ ,  $1 \text{ g/cm}^3$ ).

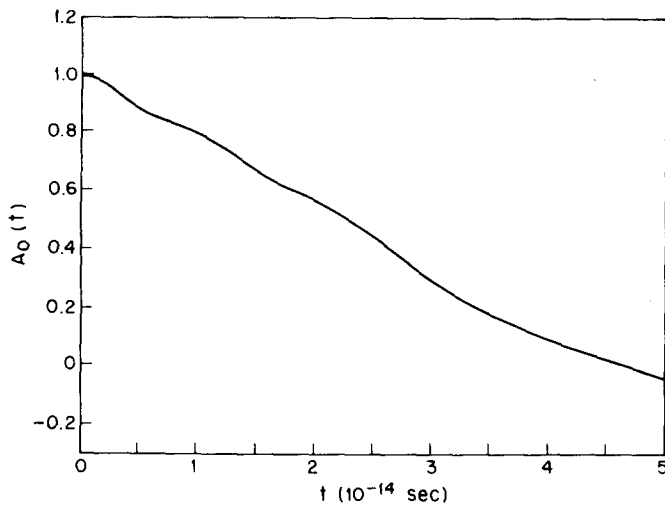


FIG. 8. Initial behavior of the oxygen velocity autocorrelation function. The time scale has been dilated by a factor 10 in comparison with Fig. 7.

The velocity autocorrelation function for hydrogens,  $A_H(t)$ , appears in Fig. 9. The vibrational amplitudes of these atoms of course are considerably larger than those of the oxygens. Therefore it should come as no surprise that what appears as minor undulation in  $A_O(t)$ , Fig. 8, has been amplified into well-developed maxima and minima in  $A_H(t)$ , Fig. 9. This marked vibrational structure is superposed on longer molecular rotational and librational contributions.

Fourier cosine transforms of the velocity autocorrelation functions provide power spectra for the nuclear motions

$$\Phi_\alpha(\omega) = \int_0^\infty A_\alpha(t) \cos(\omega t) dt. \quad (5.3)$$

These quantities offer a tool for studying the way that molecular normal modes of vibration broaden into bands as the molecules are brought together in a condensed phase. In order to produce accurate predictions of this type, longer dynamical runs would probably be required than the one on which we base this paper. Nevertheless, we have employed the available dynamics to give an idea of qualitative trends. By examining  $\Phi_H$ , we find that the symmetric bend mode on the average shifts upward in frequency; its broad band seems centered at about  $1475 \text{ cm}^{-1}$ , compared to the value  $1369 \text{ cm}^{-1}$  in Table I. By contrast, the stretch modes (which occur at  $3805 \text{ cm}^{-1}$  and  $4266 \text{ cm}^{-1}$  for separate molecules) seem to shift downward to a pair of broad overlapping bands centered near  $2900 \text{ cm}^{-1}$  and  $3500 \text{ cm}^{-1}$ . To the extent that comparison with real water infrared bands is valid, note that the symmetric bend shifts upward  $50 \text{ cm}^{-1}$ , and the stretch modes downward  $\approx 300 \text{ cm}^{-1}$ , as molecules condense to form the real room-temperature liquid.<sup>22</sup>

Mean-square displacements were monitored during the course of the molecular dynamics for both particle species. These displacements yield self-diffusion constants in the long time limit:

$$D \sim \langle [\Delta r_\alpha(t)]^2 \rangle / 6t. \quad (5.4)$$

Under conditions for which all water molecules remain undissociated, we would have  $D_O = D_H$ , while appreciable dissociation would doubtless lead to  $D_O < D_H$ . With the available short dynamical sequence, the formal diffusion constants are found to be

$$\begin{aligned} D_H &= 0.87 \times 10^{-5} \text{ cm}^2/\text{sec}, \\ D_O &= 0.73 \times 10^{-5} \text{ cm}^2/\text{sec}. \end{aligned} \quad (5.5)$$

We know from other evidence that the molecules have remained intact. The discrepancy between the values (5.5) has its explanation in the fact that rotational relaxation is far from complete over the short dynamical run. Consequently, the hydrogens are still subject to a delocalizing rotational diffusion that hardly affects the oxygens (each of which is nearly coincident with its molecular center of mass). If it had been possible to run the molecular dynamics for an order of magnitude longer,  $D_H$  and  $D_O$  should have become substantially identical.

The experimental value of the self-diffusion constant for water at  $22^\circ \text{C}$  is about  $2.1 \times 10^{-5} \text{ cm}^2/\text{sec}$ .<sup>23</sup> Although one must be cautious in the interpretation of numbers such as (5.5) based on limited dynamical information, it seems safe to conclude that molecules are diffusing too slowly in the present version of central force water. Subsequent changes in the potentials  $V_{HH}$ ,  $V_{OH}$ , and  $V_{OO}$  to improve the model should take this conclusion into account.

## VI. DISCUSSION

The present exploratory study seems to justify further attention to central force models for water. The principal goals originally set for construction of these models have been met, namely, that central forces alone can cause formation of stable molecules, and that these molecules can be induced subsequently to form a hydrogen-bond network with roughly tetrahedral coordination. But before attempting to carry out exhaustive molecular dynamics studies for a wide variety of thermodynamic

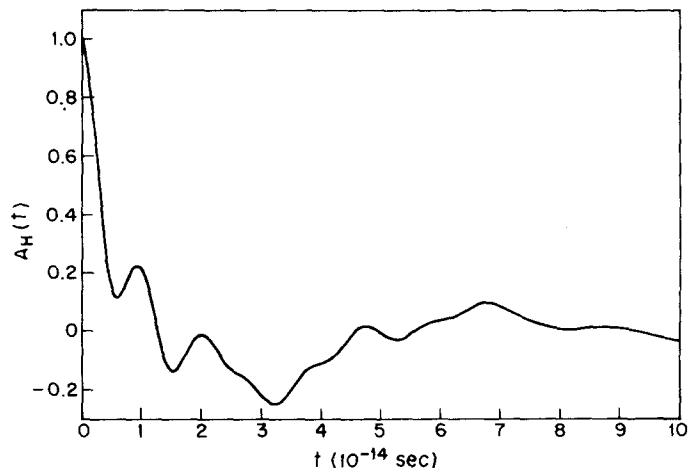


FIG. 9. Hydrogen velocity autocorrelation function for the central force model ( $22^\circ \text{C}$ ,  $1 \text{ g/cm}^3$ ).

states, it would be wise first to improve upon the specific potential functions (2.1)–(2.3).

The weakness noted earlier for the present functions, that a stable minimum exists for linear molecules, can be rectified by the simple expedient of lowering the  $V_{OH}$  curve near its minimum by several kcal/mole. This change can be introduced without affecting the curvature value (2.4) at that minimum. The result will be an increased energy cost attached to the O–H bond lengthening that accompanies the linearization. Similarly, the  $V_{HH}$  “step” at 2.0 Å could be moved outward slightly to achieve the same goal.

We have learned in the present study that the distribution of nearest-neighbor pairs of oxygens is too narrow. Therefore, modifications in  $V_{HH}$ ,  $V_{OH}$ , and  $V_{OO}$  should jointly be sought, so that the net interaction between two molecules in a linear hydrogen bond has greater breadth near its minimum. At the same time, the O–O separation of the minimum should not be allowed to shift significantly. If the molecules were given greater configurational freedom in this manner, a likely extra advantage would be a rise in the self-diffusion constants.

We have observed that the mean intermolecular binding energy is somewhat too small in our central force model. Probably related to this is the fact that the pressure  $p$  is too large; for the present simulation,

$$p/c_0 k_B T = 2.6 \pm 0.1 \quad (6.1)$$

( $c_0$  is the number density of oxygens), rather than a value close to zero to agree with experiment. One of several ways to make molecules bind more strongly would be to increase the electrostatic charge magnitudes on both oxygen and hydrogen particles. Although this would destroy the agreement between measured and modelled dipole moments of isolated molecules, it would be in accord with suggestions that water molecules in condensed phases bear considerably enhanced dipole moments.<sup>24</sup>

In the future, it will be important to produce more precise velocity autocorrelation functions  $A_\alpha(t)$  and power spectra  $\Phi_\alpha(\omega)$ , to sharpen the tentative observations offered in Sec. V. At the same time, dynamical information from the simulations could be converted to the wavelength and frequency-dependent dielectric function  $\epsilon(k, \omega)$ , for which formulas are available.<sup>12</sup> This would permit more direct comparison of the central force models with reality, using measured infrared absorption bands.

Water offers a particularly severe test of the ability of central force models to represent polyatomic liquids. Since it now appears likely that this general approach will offer valuable insights into the molecular nature of that substance, attention should be turned to analogous substances as well. Obvious candidates are HF, NH<sub>3</sub>, and CH<sub>4</sub>, and it is doubtful if any one of these cases would present a more formidable challenge than the one already met. It would be useful not only to apply the resulting central force models to fluid states, but to

apply them as well to the investigation of dynamical properties of the corresponding crystals.

## APPENDIX

The details of the theory of Ewald summations are well known and will not be repeated here; the analytical expressions are displayed for instance in recent paper by Lantelme *et al.*,<sup>25</sup> where a molecular dynamics study of molten salts is reported. We shall only mention certain technical details of interest.

With cubic boundary conditions, the Ewald sum has full cubic symmetry so that  $1/8$ th of the cube essentially spans the whole cube. We have divided half the box length,  $L/2$ , into 30 equal parts and for  $0 \leq z \leq y \leq x \leq L/2$  constructed a mesh of 4960 ( $= 30 \times 31 \times \frac{32}{3}$ ) points at which the Ewald sum, its gradient (3 components), and second derivative (6 components) are evaluated with high accuracy and stored once for all. Given the position vectors  $\mathbf{r}_i, \mathbf{r}_j$  of a pair of particles, we first construct the correct minimum image vector corresponding to  $\mathbf{r}_i - \mathbf{r}_j$  and then use a suitable table lookup and interpolation procedure to calculate the potential and the force between the two particles.

It is probably unnecessary to use a fine mesh of 4960 points, and one composed of 680 ( $= 15 \times 16 \times \frac{17}{2}$ ) is likely sufficient. Tests are being conducted to justify this reduction. If this coarse mesh is found to be sufficient, it will considerably reduce computer memory requirements.

Lastly, let  $V(\mathbf{r})$  denote the Ewald sum for the vector  $\mathbf{r}$ . Actually, the reciprocal quantity  $\varphi(\mathbf{r}) = 1/V(\mathbf{r})$  and its derivatives (first and second) are tabulated and stored. The interpolation procedure thus works on  $\varphi$  and its derivatives, and the the conversion to  $V$  and its derivatives is made. This has some advantage, since  $\varphi$  varies somewhat more smoothly than  $V$ .

\*Part of the work carried out at the Argonne National Laboratory was supported by the U. S. Atomic Energy Commission.

- <sup>1</sup>A. Rahman and F. H. Stillinger, *J. Chem. Phys.* **55**, 3336 (1971).
- <sup>2</sup>F. H. Stillinger and A. Rahman, *J. Chem. Phys.* **57**, 1281 (1972).
- <sup>3</sup>F. H. Stillinger and A. Rahman, *J. Chem. Phys.* **60**, 1545 (1974).
- <sup>4</sup>G. N. Sarkisov, V. G. Dashevsky, and G. G. Malenkov, *Mol. Phys.* **27**, 1249 (1974).
- <sup>5</sup>H. Kistenmacher, H. Popkie, E. Clementi, and R. O. Watts, *J. Chem. Phys.* **60**, 4455 (1974).
- <sup>6</sup>V. G. Dashevsky and G. N. Sarkisov, *Mol. Phys.* **27**, 1271 (1974).
- <sup>7</sup>R. O. Watts, E. Clementi, and J. Fromm, *J. Chem. Phys.* **61**, 2550 (1974).
- <sup>8</sup>A. Rahman and F. H. Stillinger, *J. Am. Chem. Soc.* **95**, 7943 (1973).
- <sup>9</sup>D. Hankins, J. W. Moskowitz, and F. H. Stillinger, *J. Chem. Phys.* **53**, 4544 (1970); erratum: *J. Chem. Phys.* **59**, 995 (1973).
- <sup>10</sup>B. R. Lentz and H. A. Scheraga, *J. Chem. Phys.* **58**, 5296 (1973).
- <sup>11</sup>F. H. Stillinger, *Adv. Chem. Phys.* **31**, 1 (1975).
- <sup>12</sup>H. L. Lemberg and F. H. Stillinger, *J. Chem. Phys.* **62**, 1677 (1975).
- <sup>13</sup>K. Huang, *Statistical Mechanics* (Wiley, New York, 1963),

Chaps. 16–17.

<sup>14</sup>The potential set displayed in Refs. 11 and 12 also possesses a relative minimum for a linear arrangement of the three atoms, but at *higher* energy than the proper bent configuration.

<sup>15</sup>We have used the IBM 360/195 located at the Argonne National Laboratory.

<sup>16</sup>A. H. Narten, M. D. Danford, and H. A. Levy, *Discuss. Faraday Soc.* **43**, 97 (1967).

<sup>17</sup>A. H. Narten and H. A. Levy, *Science* **165**, 447 (1969).

<sup>18</sup>A. H. Narten, ONRL Rep. No. ONRL-4578, July 1970.

<sup>19</sup>A. H. Narten, *J. Chem. Phys.* **56**, 5681 (1972).

<sup>20</sup>D. Eisenberg and W. Kauzmann, *The Structure and Properties of Water* (Oxford U.P., New York, 1969), p. 207.

<sup>21</sup>B. J. Alder and T. E. Wainwright, *Phys. Rev. Lett.* **18**, 988 (1967).

<sup>22</sup>Reference 20, p. 229.

<sup>23</sup>K. T. Gillen, D. C. Douglass, and M. J. R. Hoch, *J. Chem. Phys.* **57**, 5117 (1972).

<sup>24</sup>Reference 20, pp. 191–194.

<sup>25</sup>F. Lantelme, P. Turq, B. Quentrec, and J. Lewis, *Mol. Phys.* **28**, 1537 (1974).